International Journal of Nanomedicine

Dovepress
open access to scientific and medical research

Open Access Full Text Article

ORIGINAL RESEARCH

Anti-Tumor Efficacy of an Adjuvant Built-In Nanovaccine Based on Ubiquitinated Proteins from Tumor Cells

This article was published in the following Dove Press journal:
International Journal of Nanomedicine

Fang Huang[1,*]
Jinjin Zhao[1,*]
Yiting Wei[1]
Zhifa Wen[1]
Yue Zhang[1]
Xuru Wang[1]
Yanfei Shen[2]
Li-xin Wang[1]
Ning Pan[1]

[1]Department of Microbiology and Immunology, Medical School of Southeast University, Nanjing, Jiangsu Province 210009, People's Republic of China; [2]Department of Bioengineering, Medical School of Southeast University, Nanjing, Jiangsu Province 210009, People's Republic of China

*These authors contributed equally to this work

Background and Aim: We have previously identified ubiquitinated proteins (UPs) from tumor cell lysates as a promising vaccine for cancer immunotherapy in different mouse tumor models. In this study, we aimed at developing a highly efficient therapeutic adjuvant built-in nanovaccine (α-Al_2O_3-UPs) by a simple method, in which UPs from tumor cells could be efficiently and conveniently enriched by α-Al_2O_3 nanoparticles covalently coupled with Vx3 proteins (α-Al_2O_3-CONH-Vx3).

Methods: The α-Al_2O_3 nanoparticles were modified with 4-hydroxybenzoic acid followed by coupling with ubiquitin-binding protein Vx3. It was then used to enrich UPs from 4T1 cell lysate. The stability and the efficiency for the UPs enrichment of α-Al_2O_3-CONH-Vx3 were examined. The ability of α-Al_2O_3-UPs to activate DCs was examined in vitro subsequently. The splenocytes from the vaccinated mice were re-stimulated with inactivated tumor cells, and the IFN-γ secretion was detected by ELISA and flow cytometry. Moreover, the therapeutic efficacy of α-Al_2O_3-UPs, alone and in combination with chemotherapy, was examined in 4T1 tumor-bearing mice.

Results: Our results showed that α-Al_2O_3-UPs were successfully synthesized and abundant UPs from tumor cell lysate were enriched by the new method. In vitro study showed that compared to the physical mixture of α-Al_2O_3 nanoparticles and UPs (α-Al_2O_3+UPs), α-Al_2O_3-UPs stimulation resulted in higher upregulations of CD80, CD86, MHC class I, and MHC class II on DCs, indicating the higher ability of DC activation. Moreover, α-Al_2O_3-UPs elicited a more effective immune response in mice, demonstrated by higher IFN-γ secretion than α-Al_2O_3+UPs. Furthermore, α-Al_2O_3-UPs also exhibited a more potent effect on tumor growth inhibition and survival prolongation in 4T1 tumor-bearing mice. Notably, when in combination with low dose chemotherapy, the anti-tumor effect was further enhanced, rather than using α-Al_2O_3-UPs alone.

Conclusion: This study presents an adjuvant built-in nanovaccine generated by a new simple method that can be potentially applied to cancer immunotherapy and lays the experimental foundation for future clinical application.

Keywords: ubiquitinated proteins, alumina nanoparticles, cancer vaccine, combination therapy

Correspondence: Li-xin Wang; Ning Pan
Department of Microbiology and Immunology, Medical School of Southeast University, 87 Dingjiaqiao Road, Nanjing, Jiangsu Province 210009, People's Republic of China
Email lxwang@seu.edu.cn; panningmicro@aliyun.com

Introduction

Cancer immunotherapy has been ranked as one of the most exciting and popular cancer therapies due to its effectiveness and superiority in clinical trials over recent years.[1,2] Compared to the traditional cancer treatments of surgery, radiation, and chemotherapy, immunotherapy exhibits the advantages of less adverse effects and

submit your manuscript | www.dovepress.com
DovePress
http://doi.org/10.2147/IJN.S237578

more targeted ability.[3,4] Immunotherapy includes a variety of treatments such as cancer vaccines, monoclonal antibodies, gene therapies, immune checkpoint blockades, adoptive cell therapy, and so on.[1,5] Among them, therapeutic cancer vaccines are receiving more and more attention attributing to the recent success stories in the clinical treatment of tumors.[6–9]

Therapeutic cancer vaccines are medicines that treat cancers by training the immune system to recognize and attack cancer cells.[10] Thus, tumor-associated antigens (TAAs) which induce specific cytotoxic T lymphocytes ($CD8^+$ CTL) immune response are the vital components of cancer vaccines.[7] However, the poor immunogenicity and low response rate of TAAs limit the effectiveness of common clinical cancer vaccines.[8,11] There is an urgent need to develop vaccines that contain abundant and broad-spectrum TAAs for effective cancer immunotherapy.[12]

Recent studies have confirmed that DRibbles (defective ribosomal products-containing blebs) isolated from tumor cells with the induction of autophagy and inhibition of lysosomal/proteasomal activity are sufficient to stimulate dramatic T-cell activation and kill carcinoma cells in different tumor models such as melanoma, lung cancer, breast cancer and liver cancer.[13–19] Moreover, we have demonstrated that ubiquitinated proteins (UPs) are the critical TAA source of DRibbles which induce the anti-tumor efficacy. Therefore, different strategies for UPs enrichment have been developed to achieve a clinically safe, simply made, and environment-friendly vaccine with enhanced antitumor immune response.[19–21]

In our previous studies, we enriched UPs from tumor cells after proteasome inhibition by Ni-NTA agarose beads conjugated with ubiquitin-binding protein Vx3. We found that the UPs have the ability to be an effective cancer vaccine. Nevertheless, those UPs are lack of highly immunogenic and the approach is time-consuming.[19,20] To optimize the therapeutic vaccine based on UPs, a CONH linker was applied in this study to couple Vx3 protein to α-Al_2O_3 nanoparticles to generate Vx3-conjugated α-Al_2O_3 nanoparticles (denoted as α-Al_2O_3-CONH-Vx3), which enriched UPs from 4T1 cancer cell lysate (α-Al_2O_3-CONH-Vx3-UPs, denoted as α-Al_2O_3-UPs) by a single centrifugation step. By using α-Al_2O_3-CONH-Vx3, Vx3 pulls UPs out of tumor cell lysate like a fishhook, and α-Al_2O_3 functions as an immune adjuvant to enhance the immunogenicity of UPs. The results showed this strategy enriched UPs more efficiently and conveniently, and the vaccine had more potent antitumor efficacy than α-Al_2O_3 mixed with UPs. The anti-tumor efficacy of α-Al_2O_3-UPs combined with chemotherapy was also investigated in this study.

Materials and Methods

Mice

Specific pathogen-free female BALB/c mice (6–8 weeks old) were purchased from the Comparative Medicine Center, Yangzhou University (Yangzhou, China). This study has been approved by the Institutional Animal Care and Welfare Committee of Southeast University. The animal welfare guidelines of the Institutional Animal Care and Welfare Committee of Southeast University were strictly followed.

Cell Culture

4T1 cells were kindly provided by Dr. Hong-Ming Hu (Providence Portland Medical Center, USA) and cultured in RPMI-1640 (HyClone) with 10% heat-inactivated fetal bovine serum (FBS; Gibco) and 50 μg/mL gentamicin (Lonza). The use of the gifted cells was approved by the institutional ethics committee. Bone marrow-derived dendritic cells (BMDCs) were generated according to previous literature.[22] Briefly, bone marrow cells were prepared from the femurs and tibias of female BALB/c mice, then cultured in RPMI 1640 supplemented with 10% FBS, 50 μg/mL gentamicin, recombinant mouse GM-CSF (20 ng/mL; PeproTech) and recombinant mouse IL-4 (10 ng/mL; PeproTech). BMDCs were harvested by cell lifters on day 7 and used for subsequent experiments. All cells were cultured at 37°C in a humidified incubator with 5% CO_2.

Expression and Purification of Vx3 Protein

Vx3 protein was expressed and purified based on our previous work.[19,20] In brief, pUbiG101-Vx3(A7)-eGFP expressing plasmid was introduced into E. coli DH5-α competent cells (Invitrogen) to induce the expression of His-Vx3-eGFP fusion protein. Next, cells were harvested and treated with lysozyme (Sigma). After sonication and centrifugation, supernatant containing Vx3 proteins was purified using Ni-NTA agarose beads at 4°C overnight. Beads were washed 3 times with native washing buffer and the purified Vx3 protein was eluted by native elution buffer (Figure S1). The protein concentration of Vx3 was quantified by Bradford Protein Assay Kit (Beyotime Biotechnology) according to the manufacturer's protocol.

Surface Modification of α-Al_2O_3 and Generation of α-Al_2O_3-CONH-Vx3[23–25]

1 mg α-Al_2O_3 nanoparticles (Sigma) and 5 mg 4-Hydroxybenzoic acid (Sigma) were dissolved in 50 mL deionized water and stirred in an oil bath at 90°C for 2 hrs, followed by centrifugation and washing with deionized water 3 times. Subsequently, 0.667 mL 1-butanol (Aladdin) was used to block the surface residual hydroxyl groups of the products in deionized water (50 mL). The reaction process was performed in an oil bath at 90°C under stirring for 2 hrs followed by washing with deionized water 3 times. Then, the product was reacted with 50 mM N-(3-Dimethylaminopropyl)-N'-ethylcarbodiimide hydrochloride (EDC; Sigma) and 100 mM N-hydroxysuccinimide (NHS; Sigma) in phosphate-buffered saline (PBS; pH 7.2) and stirred at room temperature for 2 hrs followed by washing with PBS 3 times. The obtained product through the above steps was named as α-Al_2O_3-COOH. Surface modification of α-Al_2O_3 nanoparticles was further confirmed by Fourier Transform Infrared Spectrometer (FTIR) (Nicolet iS10, Thermo Fisher). After that, the product was mixed with Vx3 proteins at 4°C overnight. After washing with PBS 3 times, the obtained α-Al_2O_3-CONH-Vx3 was then centrifugated and harvested (Figure 1A). The α-Al_2O_3 and the products acquired after each step according to Figure 1A were detected by the energy-dispersive x-ray spectroscopy (EDS) (FEI Quanta 400FEG ESEM/EDAX Genesis X4 M, FEI Company). The protein concentration of Vx3 proteins was quantified by Bradford Protein Assay Kit (Beyotime Biotechnology) according to the manufacturer's protocol. The α-Al_2O_3-CONH-Vx3 particles generated with or without 1-butanol blocking were detected by confocal microscopy. The successfully synthesized α-Al_2O_3-CONH-Vx3 was dispersed in PBS for one, two, and three weeks to detect the stability.

UPs Enrichment from Cancer Cells by α-Al_2O_3-CONH-Vx3

4T1 tumor cells grown to 80% were treated with 200nM bortezomib (Millennium Pharmaceuticals) and 20 mM ammonium chloride (Sigma) for 9 hrs. Cells were harvested and washed with PBS 3 times, followed by treatment with RIPA lysis buffer (Millipore), protease inhibitors (MCE), phosphatase inhibitors (MCE), and PR-619 (MCE) for 20 mins on ice.[20,21] Subsequently, the supernatants were collected by centrifugation at 15,000 g for 30 mins. Then, the supernatants of UPs were dripped into the α-Al_2O_3-CONH-Vx3 nanoparticles solution and stirred for 12 hrs at 4°C. The final product α-Al_2O_3-UPs were collected by centrifugation at 1000 rpm for 15 min, and the amounts of UPs enriched by α-Al_2O_3-CONH-Vx3 were calculated by the detection of the protein reduction in the cell lysate. The protein concentration of UPs was measured by BCA Protein Assay Kit (Beyotime Biotechnology) according to the manufacturer's protocol.

Western Blot Analysis

UPs were enriched from 4T1 tumor cell lysate treated with bortezomib and ammonium chloride by α-Al_2O_3-CONH-Vx3, and the whole cell lysate, unbound lysate (the supernatant after the centrifugation for α-Al_2O_3-UPs collection from the whole cell lysate) and α-Al_2O_3-UPs were collected for Western blot analysis. All the samples were mixed with SDS-PAGE loading buffer (Invitrogen) and boiled for 5 mins. Then, the samples were centrifuged at 12000 g for 10 mins and the supernatant was resolved by 12.5% SDS-PAGE (Invitrogen). Then, the proteins were transferred to a PVDF membrane, blocked by 5% dry milk for 1 hr, incubated with primary antibody overnight at 4°C, and exposed to HRP-conjugated secondary antibody for 1 hr. The membrane was revealed using West Femto Substrate Trial Kit (Thermo Fisher). The primary antibody was anti-ubiquitin antibody (1:1000, Sigma, #3933) and the secondary antibody was goat anti-rabbit IgG HRP (1:5000, eBioscience).

Transmission Electron Microscopy (TEM)

The original α-Al_2O_3 nano-particles and the final vaccine product α-Al_2O_3-UPs dispersed in PBS (0.1 mg/mL) were deposited on a carbon-coated 400 mesh Cu grids dried at 40°C and analyzed using a JEM-2100 (HITACHI).

For the biological safety evaluation, small kidney tissue pieces (~1 mm^3) were fixed in 2.5% glutaraldehyde (Servicebio) for 2–4 hrs at 4°C and washed with 0.1 M phosphate buffer (pH 7.4) 3 times for 15 mins each. Then, the samples were post-fixed with 1% osmium tetroxide for 2 hrs at room temperature and washed three times. Subsequently, the samples were dehydrated in a series of graded ethanol, exchanged through acetone and embedded in Epon 812. Thin sections (~60–80 nm) were cut and examined with an HT770 (HITACHI) TEM.

Flow Cytometry and Antibodies[26–28]

The following fluorescently labeled antibodies were used: PE/Cy7-CD11C, PE-CD45, FITC-CD4, PE-IFN-γ, PE/Cy7-CD8, FITC-CD3e, PE-CD86, APC-CD80, APC-Mouse MHC class II (I-A/I-E), PE-Mouse MHC class I (H-2Kd), Fixable viability dye eFluor 520 from eBioscience. Dead

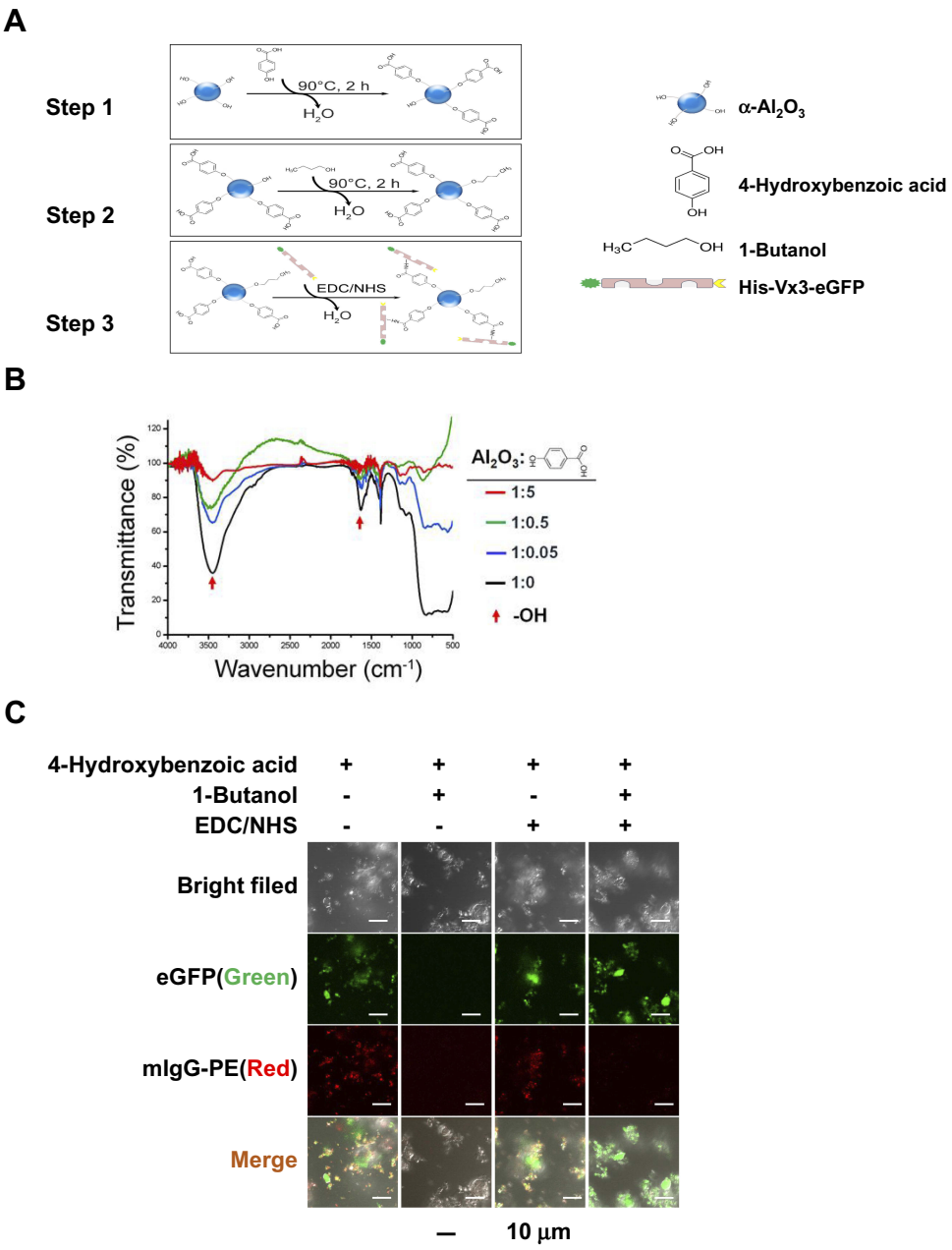

Figure 1 Surface modification of α-Al_2O_3 nanoparticles. (**A**) Schematic diagram of α-Al_2O_3-CONH-Vx3 nanoparticles. (**B**) FTIR spectra of α-Al_2O_3. (**C**) Confocal images of α-Al_2O_3-CONH-Vx3 particles generated with and without 1-butanol blockage.

cells were excluded using the Fixable viability dye eFluor 520. Data were acquired on BD FACS Calibur and analyzed by FlowJo software.

The Biological Safety Evaluation

BALB/c mice were divided randomly into two groups (n=4 per group) and then received subcutaneous injection three times with normal saline (NS) or α-Al_2O_3-UPs (containing 30 μg of UPs) at two-day intervals.[20,29] Mice were euthanized 21 days post last vaccination. Then, the major organs were dissected and collected for H&E staining analysis and TEM analysis.

BMDC Activation and Maturation Assay

On the seventh day, BMDCs (2×10^5 cells) were treated with culture medium (CM), physical mixture of α-Al_2O_3 and UPs (α-Al_2O_3+UPs) or α-Al_2O_3-UPs for 24 hrs at 37°C. BM DCs were then harvested and stained with PE/Cy7-CD11C,

PE-CD86, APC-CD80, APC-Mouse MHC class II (I-A/I-E) and PE-Mouse MHC class I (H-2Kd), followed by flow cytometry analysis.

Detection of the Specific Immune Response Elicited by α-Al_2O_3-UPs

BALB/c female mice were divided randomly into different groups (n=3 per group) and vaccinated subcutaneously three times at two-day intervals with α-Al_2O_3-UPs or controls. Seven days after the last vaccination, the splenocytes were harvested and added to 48-well plates (1×10^6 cells/well) and re-stimulated with inactivated 4T1 tumor cells treated with Mitomycin C (Sigma) or α-CD3mAb. After 48 hrs of incubation, the supernatant was collected for measuring IFN-γ by ELISA and the intracellular IFN-γ synthesized by $CD8^+$ T cells was examined by flow cytometry.

In the experiment exploring the optimal UPs dosage contained in α-Al_2O_3-UPs, BALB/c mice were divided randomly into four groups and, respectively, vaccinated with α-Al_2O_3-UPs containing 0, 10, 30 or 100 μg of UPs/mouse. In the experiment exploring the optimal ratio of splenocytes to inactivated 4T1 tumor cells, the splenocytes (1×10^6 cells/well) were, respectively, re-stimulated with 0 (1:0), 1×10^4 (1:0.01), 3×10^4 (1:0.03), 1×10^5 (1:0.1), 3×10^5 (1:0.3), or 1×10^6 (1:1) inactivated 4T1 tumor cells. In the final experiment to compare the immune responses elicited by α-Al_2O_3-UPs and α-Al_2O_3+UPs, BALB/c mice were divided randomly into three groups, and, respectively, vaccinated with NS, α-Al_2O_3+UPs (containing 30 μg UPs) and α-Al_2O_3-UPs (containing 30 μg UPs), and the ratio of splenocytes to inactivated 4T1 tumor cells is 1:0.03.

Detection of the Antitumor Efficacy of α-Al_2O_3-UPs

A 4T1 murine tumor model was established by subcutaneous injection of 4T1 tumor cells (5×10^5) into the right mammary fat pad of female BALB/c mice. Mice bearing 5-day 4T1 tumors were randomly divided into four groups (n=6 per group) and then received subcutaneously vaccination of α-Al_2O_3-UPs (containing 30 μg of UPs), α-Al_2O_3 +UPs (containing 30 μg of UPs), α-Al_2O_3-CONH-Vx3 and NS on day 5, 7, and 9, respectively, after the first inoculation of tumor cells. Whole blood samples were collected from the orbit on day 16, and the IFN-γ level in the serum was measured by ELISA.[20,21] Tumor growth and mice survival were observed every other day. Mice with tumors greater than 3000 mm^3 were euthanized. To further investigate the anti-tumor efficacy of α-Al_2O_3-UPs in combination with chemotherapeutic medication, epirubicin (EPB), BALB/c mice bearing 5-day 4T1 tumors were randomly divided into four groups (n=6 per group) and treated with or without intravenously EPB (50 μg/mouse) on day 5 combined with or without triple α-Al_2O_3-UPs vaccination or NS on day 8, 10 and 12. The IFN-γ levels in blood sera were measured by ELISA on day 19. Tumor growth was measured every other day and survival of the mice was monitored.

IFN-γ ELISA

IFN-γ production in the culture supernatant and blood serum was measured by an ELISA kit (eBioscience) following the manufacturer's guideline.

Statistical Analysis

Experimental data came from at least three independent experiments and were analyzed for statistical significance using GraphPad Prism 7 (GraphPad Software). The statistical significance of the differences between groups was evaluated by Student's *t*-test or one-way ANOVA when the data distribution was parametric. The statistical significance of the differences between groups was evaluated by Mann–Whitney's *U*-test when the data distribution was non-parametric. Kaplan-Meier survival curves were assessed by the Log-rank Mantel-Cox test. Data were expressed as the means ± SD (*=p<0.5, ** = p < 0.01, *** = p < 0.001, **** = p <0.0001) and P < 0.05 was considered significant.

Results

Surface Modification of α-Al_2O_3

The α-Al_2O_3 nanoparticles were synthesized conforming to the schematic diagram shown in Figure 1A. In order to link Vx3 protein to α-Al_2O_3 nanoparticles, the nanoparticles were undergone carboxylation by 4-Hydroxybenzoic acid (denoted as α-Al_2O_3-COOH). Surface modification of α-Al_2O_3 nanoparticles was confirmed by FTIR. The FTIR spectra of α-Al_2O_3 (Figure 1B) showed a strong and broad absorption peak at ~3448 cm^{-1}, which corresponded to the stretching vibration of hydrogen-bonded OH. Meanwhile, the sharp absorption peak was at ~1632 cm^{-1}, which revealed the scissoring vibration of adsorbed water. After the reaction between α-Al_2O_3 and different proportions of 4-Hydroxybenzoic acid, the above two absorption peaks

clearly reduced. The α-Al_2O_3 and the products acquired after each step according to Figure 1A were detected by the EDS and the EDS results (Figure S2) showed that C and N elements were detected in α-Al_2O_3-CONH-Vx3 but not in α-Al_2O_3.[30] Many more C elements were detected on modified α-Al_2O_3 nanoparticles after the reaction with 4-Hydroxybenzoic acid and the 1-butanol. Many more C and N elements were detected on modified α-Al_2O_3 nanoparticles after covalently linked with Vx3 proteins, which suggested the successful modification of α-Al_2O_3 nanoparticles. Notably, the absorption peak of OH maximum reduced when the ratio of α-Al_2O_3 with 4-Hydroxybenzoic acid was 1:5. These results suggested that α-Al_2O_3 was successfully modified with 4-Hydroxybenzoic acid, even when an excess of 4-Hydroxybenzoic acid was used to modify α-Al_2O_3, some of the hydroxyl groups remained. To test if proteins other than Vx3 could be absorbed on the 4-Hydroxybenzoic acid-modified α-Al_2O_3 nanoparticles, IgG-PE was added as irrelevant protein after Vx3 conjugation. The confocal microscopy results suggested the successful conjugation of Vx3 (indicated by green fluorescence) as well as the absorption of irrelevant protein IgG-PE (indicated by red fluorescence, Figure 1C, column 1). Therefore, 1-butanol was used to block the surface residual hydroxyl groups of α-Al_2O_3-COOH (Figure 1A, step 2). No red fluorescence was observed after 1-butanol blockage (Figure 1C, column 4), which indicates protein adsorption on α-Al_2O_3-COOH is effectively blocked.

Generation and Characterization of α-Al_2O_3-CONH-Vx3

The α-Al_2O_3-COOH was mixed with Vx3 protein at different ratios at 4°C overnight, and the covalent binding between α-Al_2O_3-COOH and Vx3 protein was detected by fluorescence microscopy. With the increase of Vx3 protein added to 1 mg α-Al_2O_3-COOH, the fluorescence intensity of the ligation product gradually increased, indicating that the Vx3 protein was successfully coupled to α-Al_2O_3-COOH (Figure 2A). The results also showed that a maximum of 50 μg Vx3 protein could be coupled to 1 mg of α-Al_2O_3-COOH (Figure 2B). Therefore, a 50 μg: 1 mg ratio of Vx3 protein to α-Al_2O_3−COOH was used in the following experiments. The stability of α-Al_2O_3-CONH-Vx3 was then tested by detecting the fluorescence intensity after storage at 4°C for one, two and three weeks. The results show that the synthesized α-Al_2O_3-CONH-Vx3 is stable at 4°C for at least 2 weeks (Figure 2C).

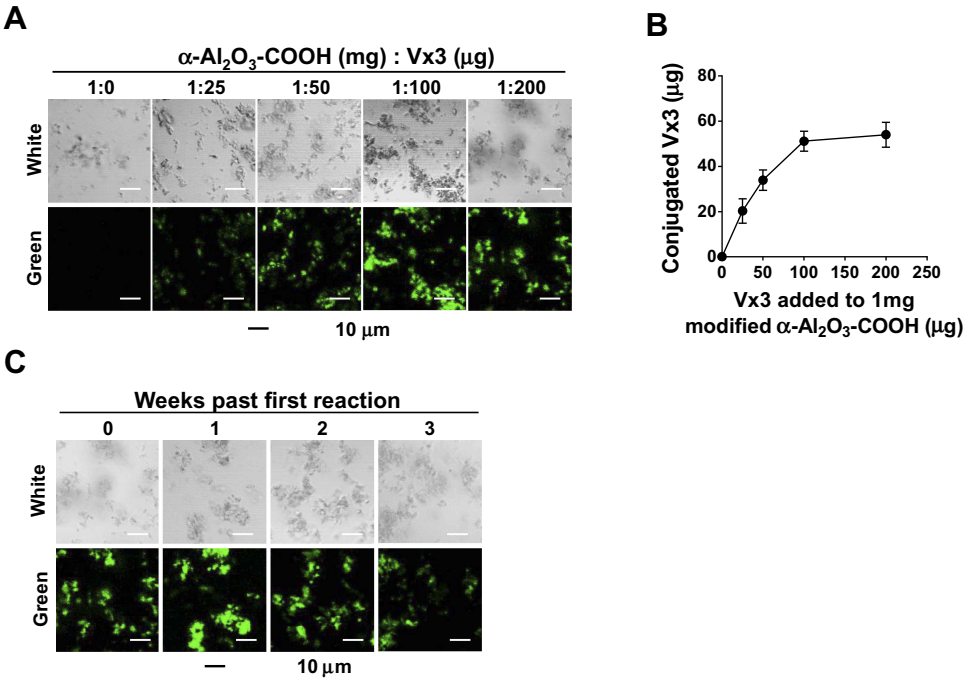

Figure 2 Vx3 proteins were coupled to α-Al_2O_3-COOH successfully. (**A**) Fluorescence diagrams of α-Al_2O_3-COOH coupled with different amounts of Vx3 proteins. (**B**) Connection between the amount of conjugated Vx3 and the amount of Vx3 added to 1 mg α-Al_2O_3-COOH. The protein concentration of Vx3 was quantified by Bradford Protein Assay. Data (means ± SD) are representative of three independent experiments results. (**C**) Fluorescence diagrams of α-Al_2O_3-CONH-Vx3 stored at 4°C for one, two, and three weeks after synthesis.

UPs Enrichment from 4T1 Tumor Cells by α-Al_2O_3-CONH-Vx3

4T1 tumor cell lysate, α-Al_2O_3-CONH-Vx3 andα-Al_2O_3-UPs was prepared according to the Materials and methods. SDS-PAGE analysis (Figure 3A) showed that equal amounts of proteins from the whole cell lysate (lane 2), unbound lysate (lane 3) and α-Al_2O_3-UPs (lane 4) were loaded. The levels of ubiquitin (Figure 3B) in the whole cell lysate (lane 2), unbound lysate (lane 3) and α-Al_2O_3-UPs (lane 4) were measured by Western blot. The results showed that the level of ubiquitin protein in α-Al_2O_3-UPs (lane 4) was markedly higher than that in the whole cell

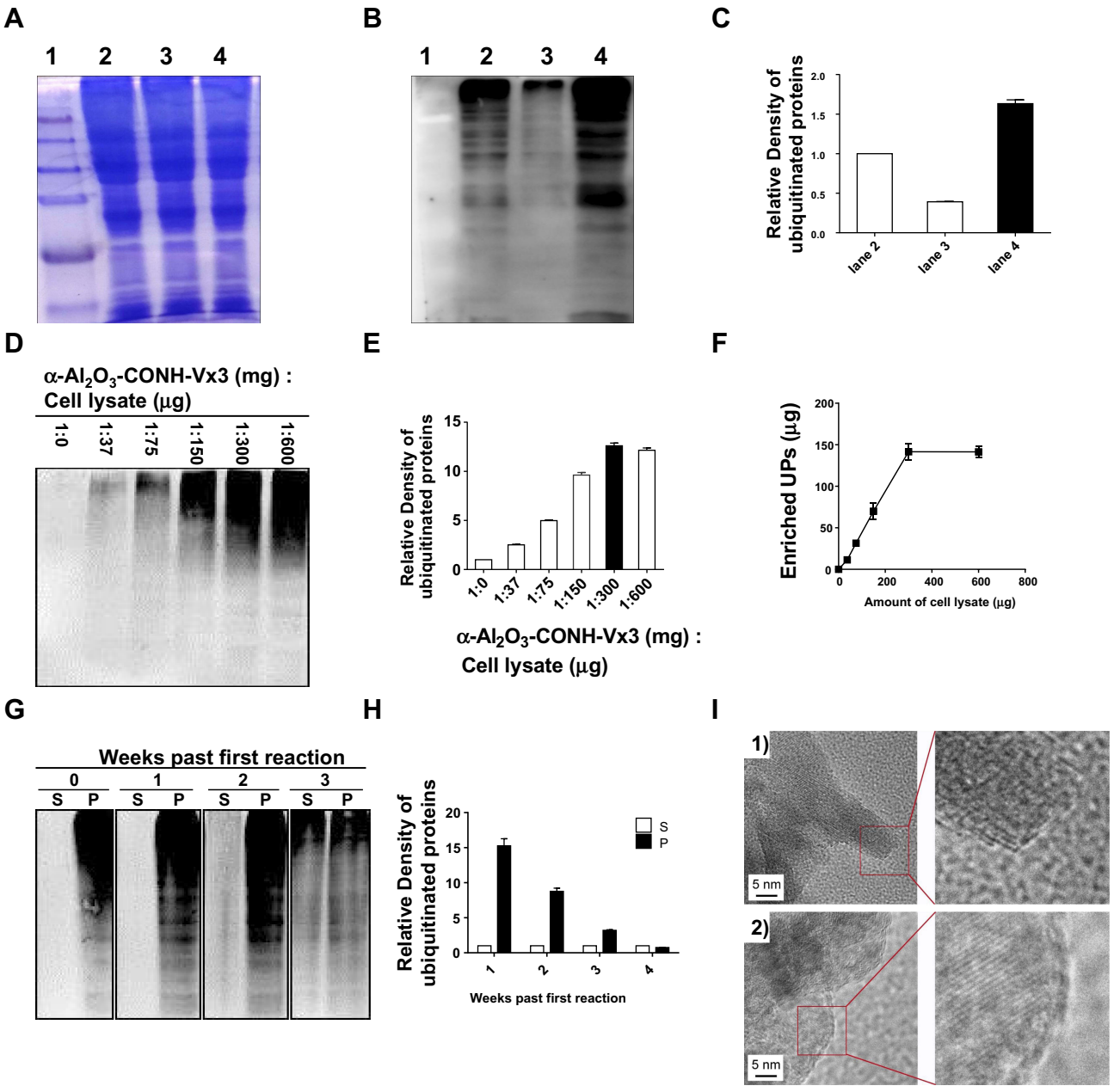

Figure 3 Enrichment of UPs by α-Al_2O_3-CONH-Vx3. (**A**) α-Al_2O_3-CONH-Vx3 was used to enrich ubiquitinated proteins from 4T1 tumor cell lysate treated with bortezomib and ammonium chloride. Molecular weight marker is represented by lane 1. The equal amounts of proteins (20 μg) from the whole cell lysate (lane 2), unbound lysate (lane 3) and α-Al_2O_3-UPs (lane 4) were loaded on 12.5% SDS PAGE gel. (**B**) Molecular weight marker is represented by lane 1. Anti-ubiquitin antibody was used to detect the ubiquitin in the whole cell lysate (lane 2), unbound lysate (lane 3) and α-Al_2O_3-UPs (lane 4) by Western blot analysis. (**C**) The relative intensities of (**B**) (normalized with lane 2). (**D**) Western blot analysis was used to detect UPs enriched by α-Al_2O_3-CONH-Vx3 after reacting with different amounts of cell lysate. (**E**) The relative intensities of (**D**) (normalized with lane 1:0). (**F**) Connection between the amount of UPs and the amount of cell lysate added to 1 mg α-Al_2O_3-CONH-Vx3. The protein concentration of UPs were quantified by BCA Protein Assay. (**G**) Western blot analyses of UPs in supernatant (S) and precipitate (P) after one, two, and three weeks of the first reaction. (**H**) The relative intensities of (**G**) (normalized with the corresponding supernatant in each group). (**I**) TEM images of constructs on (1) α-Al_2O_3 and (2) Al_2O_3-UPs. Data (means ± SD) are representative of three independent experiments results.

lysate (lane 2) and in the unbound lysate (lane 3) when the same amount of total protein was loaded. The results indicated that α-Al_2O_3-CONH-Vx3 is an efficient tool for the enrichment of UPs from tumor cell lysate (Figure 3B). The gray level analysis results are showed in Figure 3C. To show the background UPs in α-Al_2O_3-CONH-Vx3, α-Al_2O_3-CONH-Vx3 nanoparticles were divided into two equal halves. One half was used to enrich UPs from tumor lysate to produce α-Al_2O_3-UPs, which along with the other half of α-Al_2O_3-CONH-Vx3 was prepared for Western blot analysis. The results showed that there are much more UPs in α-Al_2O_3-UPs than in Al_2O_3-CONH-Vx3, indicating that most of the UPs in α-Al_2O_3-UPs comes from 4T1 tumor lysate (Figure S3). To investigate the capability of α-Al_2O_3-CONH-Vx3 recruiting UPs, different amounts of cell lysate were added to 1 mg of α-Al_2O_3-CONH-Vx3. Western blot analysis indicated that the amounts of enriched UPs were in proportion to the amount of 4T1 cell lysate added to α-Al_2O_3-CONH-Vx3 until 300 μg of lysate was added. Increasing the amount of cell lysate over 300 μg would not significantly enhance the UPs captured in the nanoparticles (Figure 3D). And the gray level analysis results are shown in Figure 3E. The same result was obtained by calculating the concentration difference of cell lysate before and after the reaction. UPs were in proportion to the amount of 4T1 cell lysate added to α-Al_2O_3-CONH-Vx3, and 1 mg α-Al_2O_3-Vx3 was able to recruit up to 150 μg of UPs (Figure 3F). Therefore, to generate the α-Al_2O_3-UPs vaccine, 300 μg of lysate was added to 1 mg of α-Al_2O_3-CONH-Vx3 in the following experiments. These results suggested that the α-Al_2O_3-CONH-Vx3 could enrich UPs from tumor cell lysate effectively. Since the stability of cancer vaccines is very important in clinical applications, we stored α-Al_2O_3-UPs suspension in PBS at 4°C for one, two, and three weeks to test its stability. The results of Western blot analysis showed that two weeks after storage, only a small proportion of UPs was detected in the supernatant, and the UPs in the precipitate scarcely reduced. These results revealed that α-Al_2O_3-UPs could be stably suspended in PBS at 4°C for two weeks (Figure 3G). Moreover, the gray level analysis results are shown in Figure 3H. Furthermore, the α-Al_2O_3 and α-Al_2O_3-UPs were observed by TEM. The results showed that the α-Al_2O_3 has a smooth surface with distinct lattices on it (Figure 3I, 1). When it was coupled with UPs, the surface was covered with an amorphous layer (Figure 3I, 2). These results demonstrate that UPs from cell lysate could be effectively enriched by α-Al_2O_3-CONH-Vx3.

The Biological Safety Evaluation of α-Al_2O_3-CONH-UPs

BALB/c mice were divided randomly into two groups (n=4 per group) and then received subcutaneous injection three times with NS or α-Al_2O_3-UPs (containing 30 μg of UPs) at two-day intervals. Mice were euthanized on day 21 and the organs were collected for histopathological analysis. Morphologies of the hearts, livers, spleens, lungs, and kidneys after H&E staining showed that there were no marked pathological changes in both vaccine group and NS group (Figure S4A). Moreover, TEM was used to study the ultrastructure of kidneys. The results indicated no pathological change of kidneys in both two groups (Figure S4B). Therefore, α-Al_2O_3-UPs exhibits a good safety profile as a nano vaccine.

Activation and Maturation of Dendritic Cells Stimulated by α-Al_2O_3-UPs in vitro

The activation and maturation of DCs are crucial for the induction of CTL responses. To test the ability of α-Al_2O_3-UPs to activate DCs, BMDCs were stimulated with α-Al_2O_3 +UPs or α-Al_2O_3-UPs. The maturation markers (CD80, CD86, MHC class I, and MHC class II) on DCs were detected by flow cytometry and quantified with the mean fluorescence intensity (MFI). The results (Figure 4A) indicated that α-Al_2O_3-UPs vaccine resulted in a significantly higher upregulation of all the markers compared to other groups. The result together with findings suggests that α-Al_2O_3-UPs could directly promote the maturation and activation of DCs.

The Specific Immune Response Elicited by α-Al_2O_3-UPs Vaccination

We seek to determine whether α-Al_2O_3-UPs could trigger a specific immune response in mice. Above all, the optimal conditions to test the immune response induction were explored. Firstly, the dosage of UPs contained in the α-Al_2O_3-UPs vaccine was tested by vaccinating mice with α-Al_2O_3-UPs containing different doses of UPs (0, 10, 30 or 100 μg of UPs/mouse) three times at two-day intervals. Mice were euthanized 7 days post last vaccination and the splenocytes were harvested, followed by re-stimulating with inactivated 4T1 tumor cells or α-CD3mAb. The levels of IFN-γ in the culture supernatant were detected by ELISA. The results indicated that α-Al_2O_3-UPs vaccination can

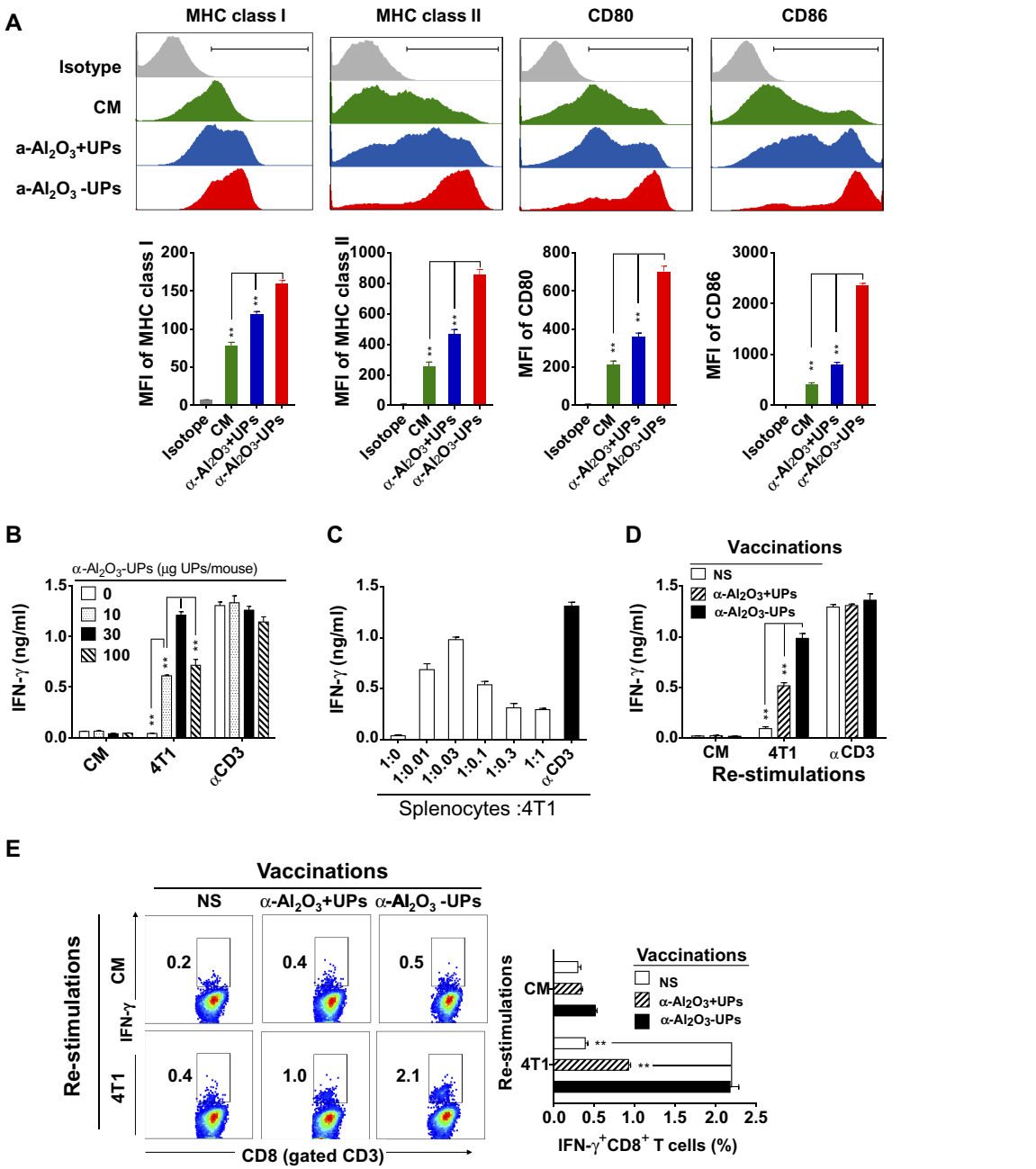

Figure 4 Effect of α-Al_2O_3-UPs on the expression of MHC class I, MHC class II, CD80, and CD86 molecule on DCs and tumor-specific immune response induced by α-Al_2O_3-UPs. (**A**) Expression analysis of MHC class I, MHC class II, CD80 and CD86 on BMDCs by flow cytometry. Cultured BMDCs were treated for 48 h with CM (green area), α-Al_2O_3 +UPs (blue area) or α-Al_2O_3-UPs (red area). (**B**) BALB/c mice (n=3 per group) were vaccinated with 0, 10, 30 or 100 μg α-Al_2O_3-UPs. The splenocytes from the vaccinated mice were then re-stimulated with inactivated 4T1 tumor cells or without stimulation (CM). αCD3-Ab stimulation was used as a positive control. IFN-γ secretion was detected by ELISA. (**C**) Splenocytes from the vaccinated mice were re-stimulated with different numbers of inactivated 4T1 tumor cells and the levels of IFN-γ were measured by ELISA. (**D**) BALB/c mice (n=3 per group) were vaccinated with NS, α- Al_2O_3+UPs (30μg) or α- Al_2O_3-UPs (30μg) via triple subcutaneous injections. The IFN-γ production by the responder cells was detected after 48 hrs by ELISA. (**E**) Flow cytometric analysis of intracellular IFN-γ produced by $CD8^+$ T cells. Data (means ± SD) are representative of three independent experiments results. **, $P < 0.01$; ns, not significant, by One-way ANOVA with the Tukey-Kramer multiple test, two-tailed unpaired *t*-test or Mann–Whitney *U*-test.

generate an effective immune response against 4T1 tumor cells in a dose-dependent manner, and 30 μg UPs induced a higher level of IFN-γ secretion than other doses (Figure 4B). Therefore, 30 μg UPs was used in the following experiments. Secondly, the ratios of splenocytes to inactivated 4T1 tumor cells were optimized and the results indicate that the optimum ratio is 1:0.03 (Figure 4C), which was then applied in the following experiments.

Subsequently, we used the above optimal conditions to detect whether α-Al_2O_3-UPs could induce a stronger anti-tumor immune response thanα-Al_2O_3+UPs. BALB/c mice were randomly divided into three groups (n=3 per group)

and immunized with NS, α-Al_2O_3+UPs (containing 30 μg of UPs) or α-Al_2O_3-UPs (containing 30 μg of UPs), respectively. Seven days after the last vaccination, mice were euthanized and the splenocytes were harvested followed by re-stimulating with inactivated 4T1 tumor cells (the ratio of splenocytes:4T1 is 1:0.03). Then, the level of IFN-γ in culture supernatant was detected by ELISA. Moreover, the splenocytes were harvested and analyzed by flow cytometry. ELISA results showed that the α-Al_2O_3-UPs group produced more IFN-γ than the α-Al_2O_3+UPs group (Figure 4D). The level of the intracellular IFN-γ synthesized by $CD8^+$ T cells examined by flow cytometry obtained the same results (Figure 4E). These data suggest that the α-Al_2O_3-UPs could induce effective specific immune responses and has the potential to become a candidate for cancer vaccines.

The Therapeutic Efficacy of α-Al_2O_3-UPs Vaccination in 4T1 Tumor-Bearing Mice

To investigate the antitumor efficacy of the α-Al_2O_3+UPs vaccine in vivo, a 4T1 murine tumor model was established. Mice bearing five-day 4T1 tumors were randomly divided into four groups. The mice then received triple subcutaneous vaccination of α-Al_2O_3-UPs, α-Al_2O_3+UPs, α-Al_2O_3-CONH-Vx3 or NS into both flanks on day 5, 7, and 9 after the first inoculation of tumor cells (Figure 5A). Blood samples from the orbit were collected from the mice 7 days after the last vaccination, and the levels of IFN-γ were measured by ELISA. The results showed that α-Al_2O_3-UPs vaccinated mice produced a higher level of IFN-γ than all the other groups (Figure 5B). Notably, vaccination with α-Al_2O_3-UPs significantly inhibited 4T1 tumor growth (Figure 5C) and prolonged the median survival time of the mice compared with the other three groups (Figure 5D).

To enhance the anti-tumor efficacy, α-Al_2O_3-UPs in combination with chemotherapeutic medication EPB was applied to the murine mammary carcinoma model, BALB/c mice bearing five-day 4T1 tumors were established and randomly divided into four groups, which were treated with or without intravenously EPB (50 μg/mouse) combined with or without subcutaneously vaccination of α-Al_2O_3-UPs on day 8, 10 and 12 (Figure 5E). Blood samples from the orbit were collected 7 days after the last vaccination, and the levels of IFN-γ were measured by ELISA. The results showed that the highest level of IFN-γ in the serum has been detected from the mice in the combination therapy group, compared to those from the other three groups (Figure 5F). Moreover, we found the combination of α-Al_2O_3-UPs and EPB more effectively inhibited 4T1 tumor growth (Figure 5G) and significantly prolonged the median survival time up to 63 days compared to 37 days for the EPB group and 52 days for the α-Al_2O_3-UPs group (Figure 5H). Therefore, these results clearly indicate that α-Al_2O_3-UPs have a potent anti-tumor efficacy in the 4T1 mammary cancer model and more effective when it combines with chemotherapy.

Discussion

Currently, cancer is a leading cause of morbidity and mortality worldwide. Cancer immunotherapy which stimulates the immune system to enhance its anti-cancer activity has been recognized as one of the indispensable pillars of treatments including surgery, chemotherapy, and radiation.[1,5] There are two crucial factors affecting the efficacy of cancer vaccine, which are TAAs and adjuvants.[31,32] TAAs expressed on cancer cells are the targets for the immune system, it can be processed and presented by professional antigen-presenting cells (pAPCs) such as DCs, and then trigger antigen-specific T cell immune responses to kill tumor cells.[22,33,34] Inactivated whole tumor cells or tumor cell lysates were kept as a source of TAAs in many therapeutic vaccines due to their numerous TAAs contained. This rich source of antigens contains multiple T-cell epitopes, which could elicit a stronger overall anti-tumor response. In addition, it could greatly diminish the chance of tumor escape compared to using single epitope vaccines.[35] However, the total clinical response rate in cancer patients following treatment with these vaccines was only 3.3%.[17,36] There are many causes of these unsatisfactory clinical outcomes. For example, the irradiated tumor cells may still have the ability to secrete immunosuppressive factors like TGF-β which could inhibit the maturation of DCs.[37,38] Similarly, some immune-suppressive molecules may be contained in tumor cell lysates.[8,39] Thus, great efforts have been made to find new sources of TAAs. Dribbles, which are isolated from tumor cells with autophagy induction and lysosomal/proteasomal activity inhibition, carry abundant ubiquitinated short-lived proteins which are almost not contained in inactivated whole-cell tumor vaccines owing to rapid degradation.[15,17,19] Our previous studies found that DRibble vaccine could efficiently cross-prime antigen-specific T cells and induce strong anti-tumor effects in several tumor models.[16–20,40] We further determined that UPs in DRibbles play the role as main TAAs

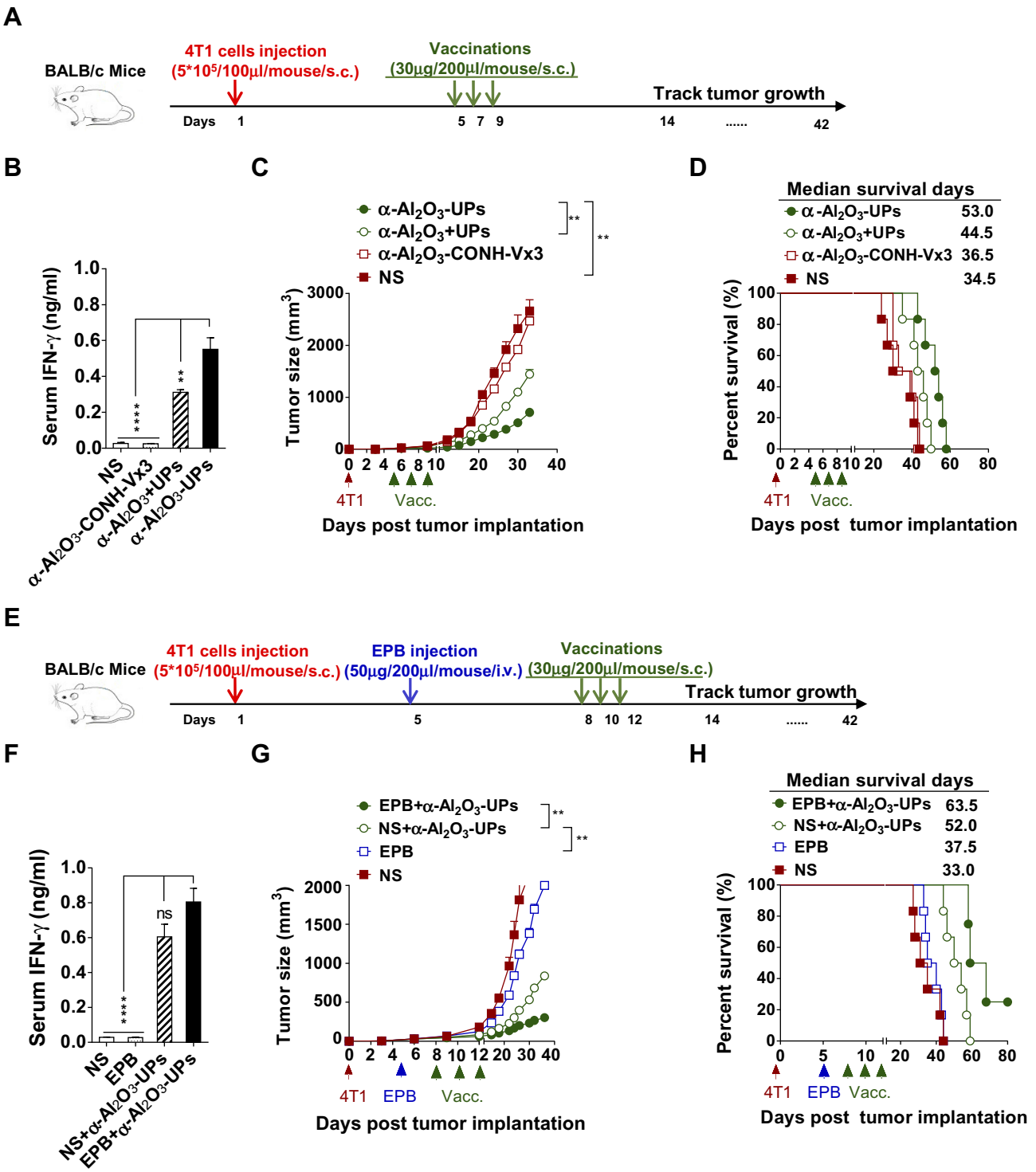

Figure 5 Anti-tumor efficacy of α-Al_2O_3-UPs vaccine in 4T1 tumor-bearing mice. (**A**) The immunization schedule for α-Al_2O_3-UPs vaccination in an established 4T1 tumor model. (**B**) The level of IFN-γ in the serum of tumor-bearing mice after treatment. (**C, D**) The tumor volume and the percent survival time of tumor burden mice with different treatments (n=6 per group). (**E**) The immunization protocol for combination therapy for the 4T1 tumor-bearing model. (**F**) The level of IFN-γ in the serum of tumor-bearing mice after treatment. (**G, H**) The tumor volume and the percent survival time of tumor-bearing mice with combination therapy (n=6 per group). Data (mean ± SD) are representative of three independent experiments results. **, P < 0.01; ****, P < 0.0001; ns, not significant, by One-way ANOVA with the Tukey-Kramer multiple test, two-tailed unpaired *t*-test or Mann–Whitney *U*-test. Kaplan-Meier survival curves were assessed by the Log-rank Mantel-Cox test.

in inducing anti-tumor efficacy, and furthermore, much more UPs could be acquired from tumor cells lysate than carried in DRibbles.[16,17,19,20]

In the previous study, we enriched UPs from tumor cell lysate using Ni-NTA agarose beads coupled with ubiquitin-binding protein Vx3. However, this Ni-NTA agarose

beads method has some significant disadvantages. Ni-NTA agarose beads are expensive for clinical application, and not environment-friendly. Moreover, the need for repeated washes in the method causes low UPs yield and high Ni-NTA agarose bead consumption. Besides, it takes 24 hrs to capture UPs from cell lysate by incubating it with the Vx3-bond agarose beads, which in combination with other steps, makes the method very time-consuming.[19,20] Therefore, a simpler, cheaper, and faster method for UPs enrichment is needed for the development of a promising vaccine.

Adjuvants are the essential components of potent vaccines which improve the immune response to vaccine antigens.[32,41] Nowadays most of the new generation vaccines are sub-unit vaccines that lack good immunogenicity and thereby essentially need adjuvants in combination to enhance immune responses.[1,42] α-Al_2O_3 adjuvants that have been approved for human use are cheap, environment-friendly, and sustainable. The α-Al_2O_3 adjuvants also have been demonstrated to have the capacity to promote the uptake and presentation of antigen by APCs and increase MHC class II expression.[40,41,43] Besides, particle size has been reported to play an important role in determining the trafficking to the lymph nodes. Only small nanoparticles can specifically target lymph nodes resident cells, which is believed as a critical step for systemic immune response generation.[44] Furthermore, recent studies showed that α-Al_2O_3 nanoparticles could boost the anti-tumor efficacy of tumor-derived autophagosomes containing limited amounts of unknown tumor-specific antigens. Hence, we choose α-Al_2O_3 nanoparticle as the adjuvant for our cancer vaccines. Moreover, instead of physically mixing antigens with α-Al_2O_3, we enriched UPs by α-Al_2O_3 linked with Vx3 proteins and generate an adjuvant built-in nanovaccine. Compared to the Ni-NTA agarose beads method, this α-Al_2O_3-CONH-Vx3 strategy greatly simplifies the enrichment procedure of UPs to one step of centrifugation which is more convenient, efficient, and significantly reduces the cost.[20]

Further results show that our vaccine with α-Al_2O_3-CONH-Vx3 strategy not only dramatically facilitates the UPs enrichment but also elicits more potent anti-tumor efficacy in comparison to the physical mixture of α-Al_2O_3 and UPs. Tumor growth was inhibited more effectively (Figure 5C) and longer survival time was achieved (median survival days, 53 vs 44.5, Figure 5D) in α-Al_2O_3-UPs group. In the experiment to detect the tumor-specific immune response induced in mouse, both $CD3^+CD8^+IFN\text{-}\gamma^+$ T cells proportion and IFN-γ secretion level were increased in the α-Al_2O_3-UPs vaccinated group when re-stimulated with inactivated tumor cells (Figure 4E), suggesting that our vaccine can induce a stronger tumor-specific immune response. In vitro experiment showed higher expression of the co-stimulatory molecules (CD80, CD86) and histocompatibility complex molecules (MHC class I, MHC class II) on DCs induced by α-Al_2O_3-UPs (Figure 4A), suggesting that the vaccine could promote the activation and maturation of DCs more effectively. Besides the results of our studies, Li et al demonstrated that when conjugated with a model peptide of OVA antigen, α-Al_2O_3 nanoparticles can serve as efficient carriers for the delivery of antigens to the autophagosome-related cross-presentation pathway in pAPCs to prime naïve T cells, and subsequently boost the anti-tumor efficacy in a B16-OVA murine model.[40] It is possible that our α-Al_2O_3 nanoparticles enhance the cross-presentation of the conjugated UPs in pAPCs and prime stronger T cell response in a similar way.

In our previous study, C=N linker was used to conjugate Vx3 to α-Al_2O_3. However, we found the vaccine generated by the C=N linker has strong autofluorescence, which leads to interference to many in vitro experiments. Compared to our previous C=N linker method, the modified α-Al_2O_3 using CONH linker method developed in this study has no autofluorescence, which is more suitable for in vitro experiments.[21] Moreover, the reagents 4-Hydroxybenzoic acid and 1-butanol used in CONH linker method are much cheaper and more easily preserved than triethoxysilane and glutaraldehyde which are used in C=N linker method.[21]

Breast cancer is a common disease with high morbidity and mortality in females worldwide, which has marked characteristics of high heterogeneous, high metastasis rate, high recurrence rate, poor survival and poor prognosis.[45] Chemotherapy remains the main therapeutic method in breast cancer, but it is often ineffective as drug resistance occurs easily and quickly for long time use. Immunotherapy strategies are becoming the newly promising therapeutic options.[46–48] Therefore, we choose 4T1 breast tumor as an animal model for stage IV human breast cancer to investigate the anti-tumor efficacy of our therapeutic cancer vaccine.[49,50]

Because of the immune escape mechanisms such as immunosuppressive environment and over-expression of inhibitory molecules, all lead to the failure of immunotherapy during cancer progression, cancer vaccines are unlikely to become a monotherapy of cancer.[51,52] Recently, cancer vaccines combined with chemotherapy have been reported

to achieve promising developments in many studies.[12,52] It has been reported that chemotherapeutic agents can induce the "immunogenic death" of tumor cells, resulting in the activation of DCs mediated by IL-12, followed by antigen cross-presentation to T cells, leading to CTLs with greater efficient cytotoxic ability.[53,54] Hence, the strategy of α-Al_2O_3-UPs vaccine combined with low dose chemotherapy was utilized to achieve a better anti-tumor effect. We found that the combination therapy further enhanced the anti-tumor efficacy of our vaccine and prolonged survival in the murine mammary carcinoma model compared to the use of α-Al_2O_3-UPs alone (Figure 5G and H). These results suggested α-Al_2O_3-UPs vaccine in combination with low dose chemotherapy may be a promising cancer combination therapy strategy due to its higher anti-tumor efficacy and lower side effects.

Conclusion

In conclusion, the α-Al_2O_3-CONH-Vx3 nanoparticles synthesized by CONH linker method can conveniently and efficiently enrich UPs from tumor cell lysate. The adjuvant built-in nanovaccine α-Al_2O_3-UPs is able to elicit a tremendous specific immune response and anti-tumor effect in a murine tumor model. Moreover, in combination with low dose chemotherapy, the anti-tumor efficacy of the vaccine could be significantly enhanced. Overall, these studies present a promising vaccine that could be applied to cancer immunotherapy and lay the experiment foundation for its clinical application.

Abbreviations

UPs, ubiquitinated proteins; TAAs, tumor-associated antigens; Dribbles, defective ribosomal products-containing blebs; BMDCs, Bone marrow-derived dendritic cells; EDC, N-(3-Dimethylaminopropyl)-N'-ethylcarbodiimide hydrochloride; NHS, N-hydroxysuccinimide; PBS, phosphate-buffered saline; TEM, Transmission Electron Microscopy; NS, normal saline; CM, culture medium; EPB, epirubicin; FTIR, fourier transform infrared spectroscopy; MFI, mean fluorescence intensity; pAPCs, professional antigen-presenting cells.

Acknowledgments

The authors are grateful for grants from the National Natural Science Foundation of China which supported this work (31970849, 31670918, and 31370895).

Author Contributions

All authors contributed to data analysis, drafting and revising the article, gave final approval of the version to be published, and agree to be accountable for all aspects of the work.

Disclosure

The authors declare that they have no conflicts of interest.

References

1. Bergman PJ. Cancer immunotherapies. *Vet Clin North Am Small Anim Pract*. 2019;49:881–902. doi:10.1016/j.cvsm.2019.04.010
2. Scheetz L, Park KS, Li Q, et al. Engineering patient-specific cancer immunotherapies. *Nat Biomed Eng*. 2019;3:768–782. doi:10.1038/s41551-019-0436-x
3. Yoo TK, Chae BJ, Kim SJ, et al. Identifying long-term survivors among metastatic breast cancer patients undergoing primary tumor surgery. *Breast Cancer Res Treat*. 2017;165(1):109–118. doi:10.1007/s10549-017-4309-2
4. Wargo JA, Reuben A, Cooper ZA, Oh KS, Sullivan RJ. Immune effects of chemotherapy, radiation, and targeted therapy and opportunities for combination with immunotherapy. *Semin Oncol*. 2015;42(4):601–616. doi:10.1053/j.seminoncol.2015.05.007
5. da Silva JL, Dos Santos ALS, Nunes NCC, de Moraes Lino da Silva F, Ferreira CGM, de Melo AC. Cancer immunotherapy: the art of targeting the tumor immune microenvironment. *Cancer Chemother Pharmacol*. 2019;84:227–240. doi:10.1007/s00280-019-03894-3
6. Lopes A, Vandermeulen G, Preat V. Cancer DNA vaccines: current preclinical and clinical developments and future perspectives. *J Exp Clin Cancer Res*. 2019;38(1):146. doi:10.1186/s13046-019-1154-7
7. McNeel DG. Therapeutic cancer vaccines: how much closer are we? *BioDrugs*. 2018;32(1):1–7. doi:10.1007/s40259-017-0257-y
8. Hu Z, Ott PA, Wu CJ. Towards personalized, tumour-specific, therapeutic vaccines for cancer. *Nat Rev Immunol*. 2018;18(3):168–182. doi:10.1038/nri.2017.131
9. Gatti-Mays ME, Redman JM, Collins JM, Bilusic M. Cancer vaccines: enhanced immunogenic modulation through therapeutic combinations. *Hum Vaccin Immunother*. 2017;13(11):2561–2574. doi:10.1080/21645515.2017.1364322
10. Song Q, Zhang CD, Wu XH. Therapeutic cancer vaccines: from initial findings to prospects. *Immunol Lett*. 2018;196:11–21. doi:10.1016/j.imlet.2018.01.011
11. Kartikasari AER, Prakash MD, Cox M, et al. Therapeutic cancer vaccines-T cell responses and epigenetic modulation. *Front Immunol*. 2018;9:3109. doi:10.3389/fimmu.2018.03109
12. Mougel A, Terme M, Tanchot C. Therapeutic cancer vaccine and combinations with antiangiogenic therapies and immune checkpoint blockade. *Front Immunol*. 2019;10:467. doi:10.3389/fimmu.2019.00467
13. Yewdell JW, Antón LC, Bennink JR. Defective ribosomal products (DRiPs): a major source of antigenic peptides for MHC class I molecules? *J Immunol*. 1996;157(5):1823–1826.
14. Li Y, Wang LX, Yang G, Hao F, Urba WJ, Hu HM. Efficient cross-presentation depends on autophagy in tumor cells. *Cancer Res*. 2008;68(17):6889–6895. doi:10.1158/0008-5472.CAN-08-0161
15. Li Y, Wang LX, Pang P, et al. Tumor-derived autophagosome vaccine: mechanism of cross-presentation and therapeutic efficacy. *Clin Cancer Res*. 2011;17(22):7047–7057. doi:10.1158/1078-0432.CCR-11-0951
16. Su S, Zhou H, Xue M, et al. Anti-tumor efficacy of a hepatocellular carcinoma vaccine based on dendritic cells combined with tumor-derived autophagosomes in murine models. *Asian Pac J Cancer Prev*. 2013;14(5):3109–3116. doi:10.7314/APJCP.2013.14.5.3109

17. Twitty CG, Jensen SM, Hu HM, Fox BA. Tumor-derived autophagosome vaccine: induction of cross-protective immune responses against short-lived proteins through a p62-dependent mechanism. *Clin Cancer Res*. 2011;17(20):6467–6481. doi:10.1158/1078-0432.CCR-11-0812
18. Xue M, Fan F, Ding L, et al. An autophagosome-based therapeutic vaccine for HBV infection: a preclinical evaluation. *J Transl Med*. 2014;12:361. doi:10.1186/s12967-014-0361-4
19. Yu G, Li Y, Cui Z, et al. Combinational immunotherapy with Allo-DRibble vaccines and Anti-OX40 co-stimulation leads to generation of cross-reactive effector T cells and tumor regression. *Sci Rep*. 2016;6:37558. doi:10.1038/srep37558
20. Aldarouish M, Wang H, Zhou M, Hu HM, Wang LX. Ubiquitinated proteins enriched from tumor cells by a ubiquitin binding protein Vx3 (A7) as a potent cancer vaccine. *J Exp Clin Cancer Res*. 2015;34:34. doi:10.1186/s13046-015-0156-3
21. Zhao J, Pan N, Huang F, et al. Vx3-functionalized alumina nanoparticles assisted enrichment of ubiquitinated proteins from cancer cells for enhanced cancer immunotherapy. *Bioconjug Chem*. 2018;29(3):786–794. doi:10.1021/acs.bioconjchem.7b00578
22. Wculek SK, Cueto FJ, Mujal AM, Melero I, Krummel MF, Sancho D. Dendritic cells in cancer immunology and immunotherapy. *Nat Rev Immunol*. 2019.
23. Fischer MJ. Amine coupling through EDC/NHS: a practical approach. *Methods Mol Biol*. 2010;627:55–73.
24. Wang C, Yan Q, Liu HB, Zhou XH, Xiao SJ. Different EDC/NHS activation mechanisms between PAA and PMAA brushes and the following amidation reactions. *Langmuir*. 2011;27(19):12058–12068. doi:10.1021/la202267p
25. Sohn YS, Lee YK. Site-directed immobilization of antibody using EDC-NHS-activated protein A on a bimetallic-based surface plasmon resonance chip. *J Biomed Opt*. 2014;19:5. doi:10.1117/1.JBO.19.5.051209
26. Holmes KL, Otten G, Yokoyama WM. Flow cytometry analysis using the Becton Dickinson FACS Calibur. *Curr Protoc Immunol*. 2002;Chapter 5:Unit 5 4.
27. Adan A, Alizada G, Kiraz Y, Baran Y, Nalbant A. Flow cytometry: basic principles and applications. *Crit Rev Biotechnol*. 2017;37(2):163–176. doi:10.3109/07388551.2015.1128876
28. Tung JW, Heydari K, Tirouvanziam R, et al. Modern flow cytometry: a practical approach. *Clin Lab Med*. 2007;27:3. doi:10.1016/j.cll.2007.05.001
29. Ren H, Zhao S, Li W, et al. Therapeutic antitumor efficacy of B cells loaded with tumor-derived autophagosomes vaccine (DRibbles). *J Immunother*. 2014;37(8):383–393. doi:10.1097/CJI.0000000000000051
30. Kostko O, Xu B, Jacobs MI, Ahmed M. Soft X-ray spectroscopy of nanoparticles by velocity map imaging. *J Chem Phys*. 2017;147(1):013931. doi:10.1063/1.4982822
31. Schijns V, Tartour E, Michalek J, Stathopoulos A, Dobrovolskiene NT, Strioga MM. Immune adjuvants as critical guides directing immunity triggered by therapeutic cancer vaccines. *Cytotherapy*. 2014;16(4):427–439. doi:10.1016/j.jcyt.2013.09.008
32. Khong H, Overwijk WW. Adjuvants for peptide-based cancer vaccines. *J Immunother Cancer*. 2016;4:56. doi:10.1186/s40425-016-0160-y
33. Dong H, Wen ZF, Chen L, et al. Polyethyleneimine modification of aluminum hydroxide nanoparticle enhances antigen transportation and cross-presentation of dendritic cells. *Int J Nanomedicine*. 2018;13:3353–3365. doi:10.2147/IJN.S164097
34. Yi Y, Zhou Z, Shu S, et al. Autophagy-assisted antigen cross-presentation: autophagosome as the argo of shared tumor-specific antigens and DAMPs. *Oncoimmunology*. 2012;1(6):976–978. doi:10.4161/onci.20059
35. Chiang CL, Benencia F, Coukos G. Whole tumor antigen vaccines. *Semin Immunol*. 2010;22(3):132–143. doi:10.1016/j.smim.2010.02.004
36. Curigliano GSG, Dettori M, Locatelli M, Scarano E, Goldhirsch A. Vaccine immunotherapy in breast cancer treatment: promising, but still early. *Expert Rev Anticancer Ther*. 2007;7:1225–1241. doi:10.1586/14737140.7.9.1225
37. Satoh E, Naganuma H, Sasaki A, Nagasaka M, Ogata H, Nukui H. Effect of irradiation on transforming growth factor-beta secretion by malignant glioma cells. *J Neuro-Oncol*. 1997;33(3):195–200. doi:10.1023/A:1005791621265
38. Huynh MLN, Fadok VA, Henson PM. Phosphatidylserine-dependent ingestion of apoptotic cells promotes TGF-beta 1 secretion and the resolution of inflammation. *J Clin Invest*. 2002;109(1):41–50. doi:10.1172/JCI0211638
39. Srivatsan S, Patel JM, Bozeman EN, et al. Allogeneic tumor cell vaccines the promise and limitations in clinical trials. *Hum Vacc Immunother*. 2014;10(1):52–63. doi:10.4161/hv.26568
40. Li H, Li Y, Jiao J, Hu HM. Alpha-alumina nanoparticles induce efficient autophagy-dependent cross-presentation and potent antitumour response. *Nat Nanotechnol*. 2011;6(10):645–650. doi:10.1038/nnano.2011.153
41. Banday AH, Jeelani S, Hruby VJ. Cancer vaccine adjuvants–recent clinical progress and future perspectives. *Immunopharmacol Immunotoxicol*. 2015;37(1):1–11. doi:10.3109/08923973.2014.971963
42. Zhang Y, Lin S, Wang XY, Zhu G. Nanovaccines for cancer immunotherapy. *Wiley Interdiscip Rev Nanomed Nanobiotechnol*. 2019;11(5):e1559. doi:10.1002/wnan.1559
43. Saxena M, Bhardwaj N. Turbocharging vaccines: emerging adjuvants for dendritic cell based therapeutic cancer vaccines. *Curr Opin Immunol*. 2017;47:35–43. doi:10.1016/j.coi.2017.06.003
44. Manolova V, Flace A, Bauer M, Schwarz K, Saudan P, Bachmann MF. Nanoparticles target distinct dendritic cell populations according to their size. *Eur J Immunol*. 2008;38(5):1404–1413. doi:10.1002/(ISSN)1521-4141
45. Scimeca M, Urbano N, Bonfiglio R, et al. Novel insights into breast cancer progression and metastasis: a multidisciplinary opportunity to transition from biology to clinical oncology. *Biochim Biophys Acta Rev Cancer*. 2019;1872(1):138–148. doi:10.1016/j.bbcan.2019.07.002
46. Edechi CA, Ikeogu N, Uzonna JE, Myal Y. Regulation of immunity in breast cancer. *Cancers (Basel)*. 2019;11:8. doi:10.3390/cancers11081080
47. Bao L, Haque A, Jackson K, et al. Increased expression of P-glycoprotein is associated with doxorubicin chemoresistance in the metastatic 4T1 breast cancer model. *Am J Pathol*. 2011;178(2):838–852. doi:10.1016/j.ajpath.2010.10.029
48. Burke EE, Kodumudi K, Ramamoorthi G, Czerniecki BJ. Vaccine therapies for breast cancer. *Surg Oncol Clin N Am*. 2019;28(3):353–367. doi:10.1016/j.soc.2019.02.004
49. Kaur P, Nagaraja GM, Zheng H, et al. A mouse model for triple-negative breast cancer tumor-initiating cells (TNBC-TICs) exhibits similar aggressive phenotype to the human disease. *BMC Cancer*. 2012;12:120. doi:10.1186/1471-2407-12-120
50. Sztalmachova M, Gumulec J, Raudenska M, et al. Molecular response of 4T1-induced mouse mammary tumours and healthy tissues to zinc treatment. *Int J Oncol*. 2015;46(4):1810–1818. doi:10.3892/ijo.2015.2883
51. Marshall HT, Djamgoz MBA. Immuno-oncology: emerging targets and combination therapies. *Front Oncol*. 2018;8:315. doi:10.3389/fonc.2018.00315
52. Ott PA, Hodi FS, Kaufman HL, Wigginton JM, Wolchok JD. Combination immunotherapy: a road map. *J Immunother Cancer*. 2017;5:16. doi:10.1186/s40425-017-0218-5
53. Wang YJ, Fletcher R, Yu J, Zhang L. Immunogenic effects of chemotherapy-induced tumor cell death. *Genes Dis*. 2018;5(3):194–203. doi:10.1016/j.gendis.2018.05.003
54. Rapoport BL, Anderson R. Realizing the clinical potential of immunogenic cell death in cancer chemotherapy and radiotherapy. *Int J Mol Sci*. 2019;20:4. doi:10.3390/ijms20040959